

THERMAL AND UV DEGRADATION OF POLYIMIDES AND SILICONES STUDIED *IN SITU* WITH ESR SPECTROSCOPY

Kenneth Rasmussen^{(1),(2)}, Günter Grampp⁽¹⁾, Marc van Eesbeek⁽²⁾, Thomas Rohr⁽²⁾

⁽¹⁾ Graz University of Technology, Institute of Physical and Theoretical Chemistry, Technikerstrasse 4/I, 8010 Graz, Austria, Tel.: +43 316 873 8721, Kenneth.Rasmussen@tugraz.at

⁽²⁾ ESA-ESTEC, Materials Space Evaluation & Radiation Effects Section, P.O. Box 299, 2200 AG Noordwijk ZH, The Netherlands, Tel.: +31 71 565 6777, Thomas.Rohr@esa.int

ABSTRACT

Thermal and UV degradation of several common space-grade polyimides and silicones was studied *in situ* using electron spin resonance (ESR) spectroscopy. With this method paramagnetic species, present in a sample, can be detected. Such species include radicals, transition metal ions and colour centres. From their various ESR signals, one may obtain concentrations and, depending on the material, also molecular structures.

In the present case, the radicals formed during thermal or UV degradation of films of the polyimides Kapton HN and Upilex S as well as of bulk samples of the DC 93-500 and Elastosil S 690 silicones were studied. By recording subsequent spectra at a sufficient rate, the time dependence of the radical concentration could be followed, allowing more detailed study of the kinetics of the degradation process.

The thermal degradation of Kapton HN was found to consist of two main processes, one being a radical termination and the other the actual degradation process. UV degradation experiments showed that the polyimides degrade at a much faster rate than the silicones.

1. INTRODUCTION

With the current development pace of new polymers having a potential for space applications, a fast screening and cost effective method for pre-selection and basic performance characterization would be very valuable. One such method shall be presented, and its general feasibility demonstrated.

Important goals were to set up an ESR facility at ESA/ESTEC and to develop a standard UV exposure test for screening purposes. With these in place, a complementary method for characterisation and space environmental performance evaluation of materials would be available.

The main method of analysis is ESR spectroscopy, which deals with the resonant microwave absorption of samples in an external magnetic field. It is similar to the better known nuclear magnetic resonance (NMR) spectroscopy, but is restricted to paramagnetic

compounds, such as organic radicals, complexes of transition metal ions and defects in crystals. This limitation, however, is also one of the strengths of the method as it can be applied very specifically.

ESR spectroscopy, where the first derivative of the microwave absorption intensity is measured as a function of the magnetic field, may be used to determine the amount of spins present in a sample. Most often, this is done by comparing the double integral owing to an unknown sample to that of a known standard. The reason for this is that the magnitude of the ESR absorption depends heavily on spectrometer settings, as well as on temperature. Furthermore, ESR spectroscopy may provide information about the general type of radicals present, via the so-called g-factor, and sometimes also their structure, if sufficient hyperfine interactions can be detected.

The idea of using ESR to study polymer degradation is not new and several investigations are reported in literature. For example, Ahn and co-workers studied the behaviour of thermally aged polyimide PMR-15 and characterised the generated radicals using conventional ESR [1, 2] as well as ESR imaging [3]. Also, in study by Blair *et al.* [4], the thermal ageing of several polysiloxane foams was investigated.

The UV degradation of Kapton H was reported by George *et al.* [5], who studied samples that been irradiated in either vacuum or air. These authors, among other things, investigated the dependence of the ESR signal on the duration of irradiation as well as on elevated temperatures and also, the stability of the generated radicals was studied. Additionally, they determined the relaxation parameters of the radicals.

Other methods which have been used to generate radicals for use in ESR studies of polyimide degradation, include γ -radiolysis [6, 7], and irradiation with accelerated protons [8] electrons [9, 10] and heavy ions [11].

Most of these, however, were conducted *ex situ*, that is the sample was exposed to a source of degradation and subsequently transferred to the ESR spectrometer for measurement. An exception is the study of the UV degradation of Kapton, along with a series of other polyimides, conducted by Hill *et al.* [12]. Here samples

were irradiated in situ in the ESR resonator and the change in radical concentration with time was monitored.

In the present work, the radicals created during the thermal or UV degradation of various polymers have been monitored during the exposure, thus providing in situ information of the on-going processes. The materials which were investigated were the polyimides Kapton HN (DuPont, USA) and Upilex S (UBE Industries, Japan) as well as the DC 93-500 (Dow Corning, USA) and Elastosil S 690 (Wacker, Germany) silicones, all being widely used in the space industry.

2. EXPERIMENTAL

2.1 The ESR Facility

A Bruker EMX ESR spectrometer, operating at X-band (9.5 GHz) and with a 100 kHz modulation frequency, was used in these investigations (Fig. 1). In this, the standard TE₁₀₂ mode resonator of Bruker is installed, with both optical window and cooling plates mounted. With this setup, temperatures from -150°C to 340°C can be reached and kept within 1°C.

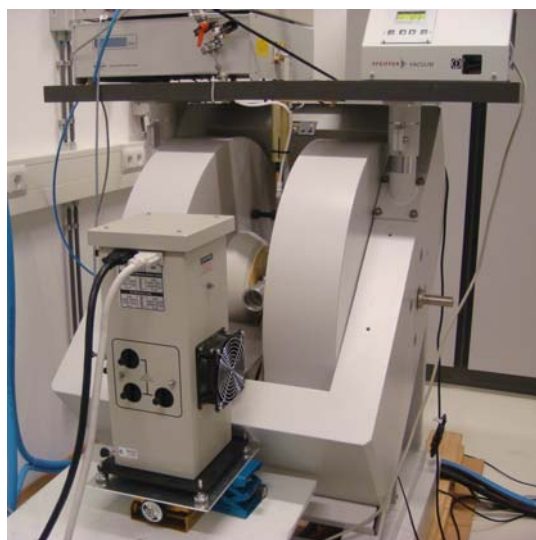


Fig. 1. The ESR facility.

The ESR sample cells consist of a sealed quartz tube of 5, 6 or 10 mm diameter, depending on the intended application, which is attached to a joint for connection to the high vacuum system.

UV-irradiation is provided by a 1000W Oriel Hg/Xe lamp which is placed in front of the ESR magnet. The output of the lamp is focused onto an adjustable lens which is attached to the resonator.

In some cases, it is desirable to reduce the intensity of the light emitted by the lamp. This is achieved by applying a simple mesh, allowing a transmission of approximately 38% of the incoming light over the whole range of wavelengths. If needed, two successive meshes can be applied, leading to a combined reduction of the light intensity to about 14% of the initial value.

2.2 Experimental Procedures

Sample preparation consisted simply of cutting the material to the desired shape and size. In the case of Kapton HN and Upilex S, 25 µm films in pieces of approximately 10-15 mm width and 30-40 mm length were used. These were rolled up and introduced into the sample tube. For the silicones, samples were cut from bulk slabs, producing rough slivers of dimension 2-3 mm × 2-3 mm × 30-40 mm.

Prior to measurements, the sample was evacuated and kept under vacuum for some time before being exposed to elevated temperature or UV. In the case of the latter, a standardised test was developed, see below, whereas for the former the duration of exposure was varied according to the response of the sample.

2.3 Standardised UV Exposure Test

As already mentioned, a major aim was to develop a standardised test, which could be applied generally in the reported and in future investigations. It is important that such a test is fast and efficient and as it was necessary to produce complete ESR spectra relatively quickly, in certain cases, compromises had to be made. To achieve the necessary signal-to-noise ratio, large, yet still reasonable, values of the modulation amplitude and microwave power were chosen, thus decreasing the spectral resolution and risking microwave saturation. Lack of resolution will have no influence on the determination of double integrals. Saturation, on the other hand will, as quantification using a standard sample is no longer straightforward.

For the test, a 30 min irradiation of the samples was decided, at the highest possible light intensity, during which an ESR spectrum was recorded approximately every 40-60 seconds

Immediately before and after the UV exposure, ESR spectra were acquired at ambient condition in order to determine the amounts of radicals present in the sample.

2.4 Data Analysis

ESR spectra were simulated using WinSim 2002 a freeware program by D. R. Duling [13]. In order to

determine the amount of radicals in a sample, the corresponding ESR spectra were integrated twice, thus arriving at quantity which is proportional to the radical concentration. This was then related to a spectrum of a standard sample of known concentration; the Bruker Strong Pitch with 1.2×10^{17} spins/cm³, or 3.3×10^{16} spins that are actually inside the ESR resonator.

The kinetic data was analysed using Origin 7 (OriginLab Corp.), providing curve fits as well as statistical analyses. In most cases, the corrected double integral, $A(t) - A(0)$, was plotted against time before fits to different theoretical models were made.

3. RESULTS AND DISCUSSION

3.1 ESR Spectra

Pristine samples of Kapton HN and Upilex S show an inherent ESR signal, due to the manufacturing process of the materials, which includes a curing period at elevated temperatures. The Kapton ESR signal showed a single line at $g = 2.0051$ with a width of $\Delta B_{pp} = 7.1$ G, which is in good agreement with literature, reporting $g = 2.005$ and $\Delta B_{pp} = 8$ G [4, 11]. For Upilex S, a single line at $g = 2.0048$ with a 5.2 G width was obtained. These line positions are consistent with oxygen or nitrogen centred radicals, as reported in literature [4, 12]. For both materials, the lines deviate from the theoretical Lorentzian and Gaussian line shapes, indicating some degree of unresolved hyperfine splitting.

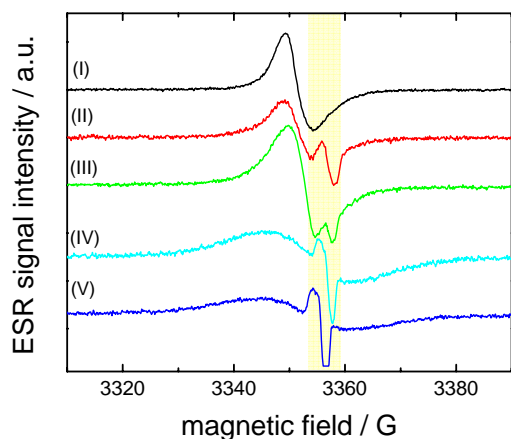


Fig. 2. ESR spectra of Kapton HN exposed to 300°C for 6 hours (I) as well as of Kapton HN (II), Upilex S (III), Elastosil S 690 (IV) and DC 93-500 (V) after 30 min UV irradiation. The marked signal owes to defects in the quartz sample cell.

Fig. 2 shows the ESR spectra of samples after their exposure to elevated temperature or UV irradiation.

The spectra of the polyimide are similar to those of the unexposed samples, albeit being more intense. For the two silicones, no signal could be detected on the unexposed samples, but UV irradiation produces broader single-line spectra than those of the polyimides. The g -factor of the DC 93-500 spectrum was 2.0034 and the line width 13.6 G, whereas $g = 2.0039$ and a width of 14.5 G were found for Elastosil S 690. Like with the polyimides, the spectra could not be fit to the theoretical shapes, indicating that also the silicones possess unresolved hyperfine interactions. Also, in all spectra of UV exposed materials, a narrow signal was seen at $g = 2.0018$. This originates from radiation induced defects in the quartz of the sample cells. However, simulations showed that the contribution of this signal to the total double integral was usually 1-3% and thus negligible. Defects of this type can be completely removed by tempering of the ESR cells and this was done after every two or three experiments.

3.2 Determination of Spin Concentrations

The amount of free radicals in each sample was determined as described earlier and can be seen in Fig 3. Note that for the silicones, despite the fact that no signals from the materials themselves were observed, the double integration of their ESR spectra led to a non-zero value, owing to the noise level and defects in the sample cells. A spectrum illustrating this can be found in Fig. 7.

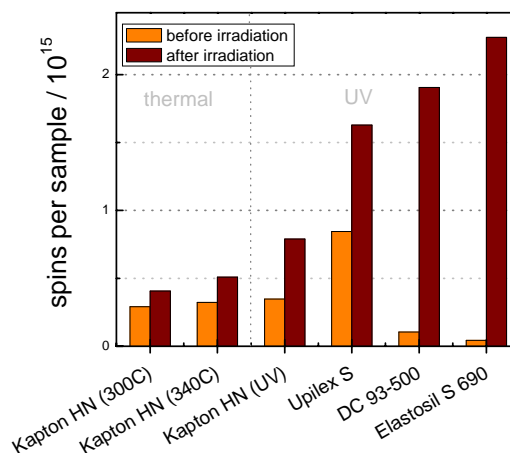


Fig. 3. Numbers of spins per sample for the different experiments.

For better comparison between the different types of samples and experiments, the results are presented in terms of spins per sample. The main reason for this is that in the UV experiments only a part of the sample

was exposed. Judging from the discolouration of the samples after irradiation, the area of exposure is approximately 20-25 mm², slightly less than that of the window of the resonator and corresponding to a volume of about 50 mm³ for the silicones.

In the thermally exposed samples, it is assumed that the radicals are formed uniformly in the material and a concentration may be calculated, arriving at 3.1×10^{17} radicals/g for the samples which were kept at 300°C for 6h in vacuum. For comparison, the PMR-15 samples of Ahn et al. showed a concentration of 6.3×10^{18} radicals/g [1] in a sample which had been kept in air at 316°C for 16h.

3.3 Power Saturation Experiments

As mentioned above, relatively high microwave powers were needed in order to ensure a sufficient signal-to-noise ratio for scan times of a minute or less. To better assess the effects from power saturation, ESR spectra were acquired at different microwave powers. For Kapton H and other polyimides such as Ultem, saturation is reported to set in at 20-100 μ W [3, 4, 9] but deviations are not expected to be severe up to at least 0.5 mW [14]. This observation is affirmed in Fig. 4, where the power saturation curves of Kapton HN and Elastasil S 690 are presented. The microwave power used in the present experiment (max. 0.6 mW) does seem to allow a small degree of saturation of the polyimides; however this is within 5% as indicated by the error bars. In the case of the silicones, saturation does not occur until at least 5 mW, raising no reasons for concerns.

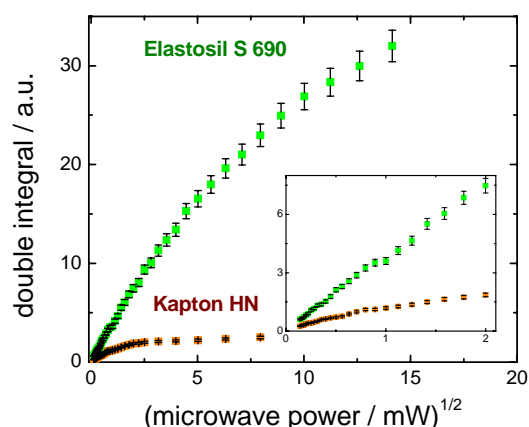


Fig 4. Power saturation curves for Kapton HN and Elastasil S 690. Error bars correspond to 5%.

3.4 Thermal Degradation of Kapton HN Films

All four materials were submitted to elevated temperatures, but even at 300°C only Kapton HN showed noticeable signs of degradation. This observation is in agreement with previously reported mass loss measurements [15, 16].

Each Kapton HN sample was heated to one of several elevated temperatures and kept at this for as long as 120 hours. At regular intervals ESR spectra were acquired and the corresponding double integrals determined. The results are shown in Fig. 5 and as it can be seen, the behaviour of Kapton HN is very different at the various temperatures. Note that here, not the corrected but the relative double integral is plotted. This is done in order to allow a better representation of the curves. Since the ESR absorption depends inversely on temperature, following a Curie-Weiss type law, direct comparison of double integrals owing to two different temperatures is not straightforward. By using the normalised values instead, this is facilitated without losing information on the chemical kinetics.

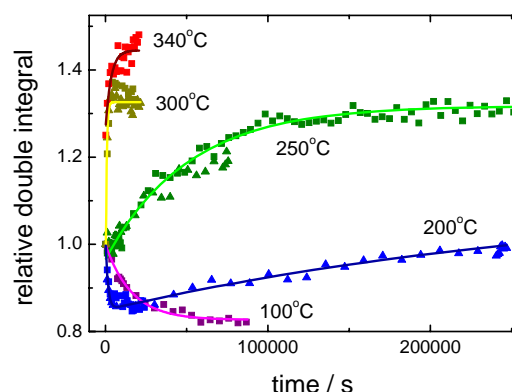


Fig. 5. Kinetic curves for the thermal decomposition of Kapton HN.

At relatively low temperatures (100°C) a first order decay described the data well, whereas at high temperatures (above 250°C) the data could be fitted to first order build-ups. At 200°C, it is clear that none of the two situations alone will describe the data sufficiently. However, using the sum of one of each kind of function, a reasonably good fit was obtained. The outcome is shown in Table 1, where k_1 denotes the rate constant of the degradation process and k_2 that of the radical decay. Both rate constants increase with higher temperatures, indicating positive activation energies, with that of the radical decay being higher.

Table 1. Experimental rate constants of thermally induced degradation reactions.

Temperature / °C	$k_1 / 10^{-5} \text{ s}^{-1}$	$k_2 / 10^{-5} \text{ s}^{-1}$
100		5.6 ± 0.8
200		62 ± 4
	0.3 ± 0.2	45 ± 7
250	2.0 ± 0.5	
	2.3 ± 0.1	
300	9 ± 1	
	16 ± 2	
340	30 ± 8	

It appears evident from the recorded data that at least two competing mechanisms are present. One is dominating at higher temperatures, causing radical generation, and a second dominates at lower temperatures leading to radical termination.

3.5 UV Degradation of Polyimide Films

UV irradiation of the polyimides showed that they could not withstand the full intensity provided by the lamp. The materials were scorched and in some cases the light burned completely through them. Therefore a mesh was used as discussed above but even with this a discolouration of the material could be seen after the exposure. It was shown by Iwata [10] that this discolouration correlates well with the amount of radicals generated in the material.

At the reduced light intensity, it was possible to kinetic curves as shown in Fig. 6.

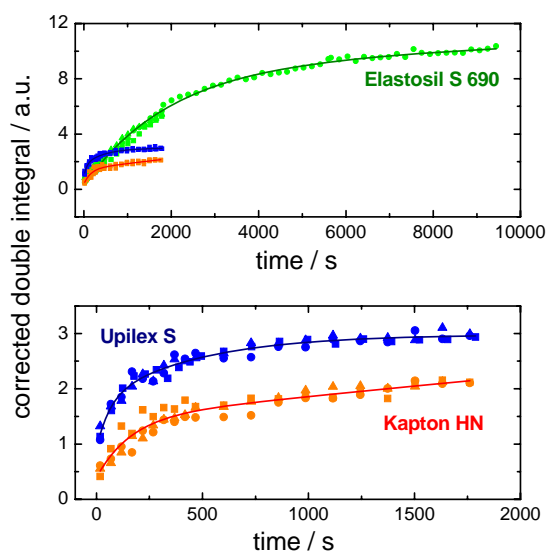


Fig. 6. Kinetic curves for Kapton HN, Upilex S and Elastosis S 690.

The data obtained in the experiments was analysed using different kinetic functions and it was found that a simple exponential increase no longer offers a sufficient description. In stead, a bi-exponential one was used and it fits the data reasonably well. This indicates that at least two degradation reactions take place simultaneously, possibly leading to the formation of different radicals. The faster of the two processes corresponded to a rate constants of $k_1 \approx 10^{-2} \text{ s}^{-1}$, while the slower had $k_2 \approx 10^{-4} \text{ s}^{-1}$, cf. Table 2 for details. Note that for Kapton HN, the rate constant of the slow process is similar to those seen in Table 1, indicating a possible thermal degradation taking place due to heating of the sample caused by the UV irradiation.

Table 2. Average experimental rate constants of UV induced degradation reactions.

Sample	$k_1 / 10^{-2} \text{ s}^{-1}$	$k_2 / 10^{-4} \text{ s}^{-1}$
Kapton HN	1.5 ± 0.4	5.9 ± 0.9
Upilex S	1.6 ± 0.3	22 ± 3
Elastosis S 690	-	4.2 ± 0.2

3.6 UV Degradation of Silicone Samples

Both silicones could be irradiated at full light intensity, leading to an acceptable level of discolouration after the 30 min exposure. For Elastosis S 690, kinetic curves similar to those mentioned previously were obtained and the radical build-up was found to be significantly slower than for the polyimides. In order to get a more complete picture of the kinetics, one of the samples was irradiated for a total of 160 minutes. Analysis of the data showed that for this material, the simple exponential model could be applied, leading to rate constants as shown in Table 2.

DC 93-500, on the other hand, behaved completely differently than the other irradiated materials. Immediately upon exposure, a comparatively large amount of radicals could be observed and within the following 2-3 minutes it decreased by about 25%, where after it remained practically constant. The rapid increase and subsequent decrease meant that it was impossible to collect enough data to reliably determine the chemical kinetics. However, the ESR spectra themselves offered additional information about the processes that take place during the degradation of this silicone. As can be seen in Fig. 7, at least two species are present during the course of the exposure. The characteristic four-line ESR spectrum of the initial one corresponds to that of a methyl containing radical, with a hyperfine splitting constant of 19.5 G and a g-factor of 2.028. The second species, which appears after about 2 minutes is the one which was described earlier, and is quite similar to that obtained for Elastosis S 690.

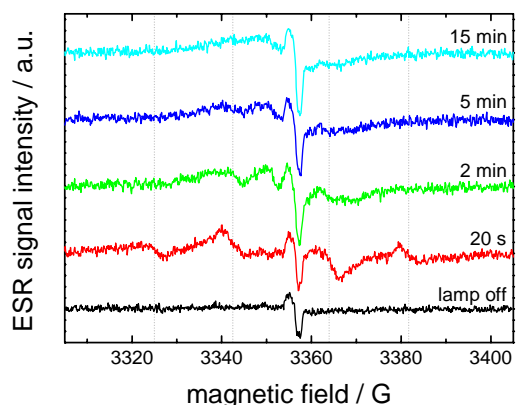


Fig. 7. ESR spectra of DC 93-500 illustrating the presence of different species throughout the experiment.

Another difference was seen in the discolouration of the two silicones during the experiments. DC 93-500 showed a relatively light discolouration, which went at least 1 mm into the material, whereas Elastosil S 690 showed a stronger discolouration mostly found at the surface of the sample. This is seen in Fig. 8, where cross-sections of two exposed samples are presented.

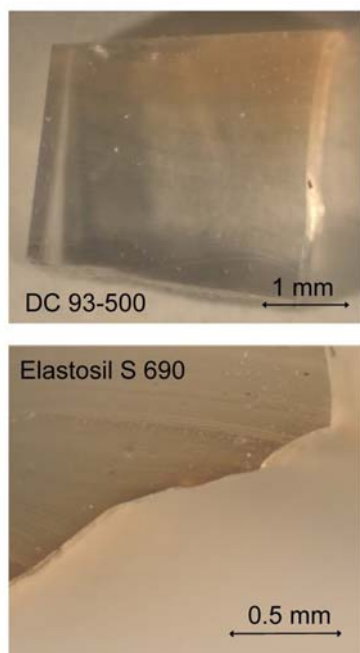


Fig. 8. Cross-sections of irradiated samples of DC 93-500 and Elastosil S 690.

An explanation of the differences in behaviour may be found in the fact that Elastosil S 690 contains phenyl groups, whereas DC 93-500 does not. The stronger and surface near discolouration is enhanced by the presence

of phenyl groups in the silicone structure. Phenyl groups are more susceptible to UV degradation than methyl groups and result in the formation of surface near degradation products exhibiting high extinction coefficients in the UV and visible spectral regions. Here as well, secondary thermal effects are possible because of the increase of absorbance and subsequently rise in temperature in the high vacuum environment.

4. CONCLUSIONS

Using the newly set-up ESR facility it was possible to gain new insights in the processes that take place during the thermal and UV degradation of polymers.

The thermal degradation experiments on Kapton HN, revealed a very interesting temperature dependence of the reaction kinetics. It is clear that two processes take place during the heating of the samples. At low temperatures, a stabilisation of the material is observed, whereas at high temperatures degradation is seen. In the intermediate region, both processes could be detected.

Within a family of similar materials a relative comparison for materials performance was possible, however, with the current method is not yet possible to gain absolute performance characteristics of materials. Future challenges involve the consideration of effected volume within the material, the formation of gradients, and the isolation of radical species that may contribute to different extent to the subsequent degradation reactions.

Overall, the ESR facility has proven to be very promising as complementary to the existing facilities and with the presented standard test will greatly assist in the evaluation of existing and future materials.

5. REFERENCES

1. Ahn, M. K., Weber, R. T., and Meador, M. A., *NASA Conf. Publ.*, **1993**, 19117, 20/1-20/11.
2. Ahn, M. K., Stringfellow, T. C., Fasano, M., Bowles, K. J., and Meador, M. A., *J. Polym. Sci., Part B: Polym. Phys.*, **1993**, 31, 831-841.
3. Ahn, M. K., Eaton, S. S., Eaton, G. R., and Meador, M. A., *Macromolecules*, **1997**, 30, 8318-8321.
4. George, M. A., Ramakrishna, B. L., and Glausinger, W. S., *J. Phys. Chem.*, **1990**, 94, 5159-5164.
5. Blair, M. W., Muenchausen, R. E., Taylor, R. D., Labouriau, A., Cooke, D. W. and Stephens, T. S., *Polym. Degrad. Stab.*, **2008**, 93, 1585-1589.
6. Zhdanov, G. S., Klinshpont, E. R., and Isakov, L. I., *Nucl. Instrum. Methods Phys. Res., Sect. B*, **2001**, 185, 140-146.
7. Devasahayam, S., Hill, D. J. T., and Connell, J. W., *Radiat. Phys. Chem.*, **2001**, 62, 189-194.

8. Artiaga, R., Chipara, M., Stephens, C. P., and Benson, R. S., *Nucl. Instrum .Methods Phys. Res., Sect.B*, **2005**, 236, 432-436.
9. Iwata, M., Imai, F., Imagawa, K., Morishita, N., and Kamiya, T., *Proc. of the 9th ISMSE*, **2003**, ESA SP-540, 617-621.
10. Iwata, M., *Proc. of the 10th ISMSE & the 8th ICPMSE*, **2006**, ESA SP-616.
11. Popok, V. N., Azarko, I. I., Khaibullin, R. I., Stepanov, A. L., Hnatowicz, V., Mackova, A. and Prasalovich, S. V., *Appl. Phys. A*, **2004**, 78, 1067-1072
12. Hill, D. J. T., Raoul, F. A., Forsythe, J. S., O'donnell, J. H., Pomery, P. J., George, G. A., Young, P. R., and Connell, J. W., *J. Appl. Polym. Sci.*, **1995**, 58, 1847-1856.
13. Duling, D. R., *J. Magn. Reson. Ser. B*, **1994**, 104, 105-110
14. Devasahayam, S., Hill, D. J. T., Pomery, P. J., and Whittaker, A. K., *Radiat. Phys. Chem.*, **2002**, 64, 299-308.
15. Semprimoschnig, C. O. A., Heltzel, S., Polsak, A. and v. Eesbeek, M., *Proc. of the 9th ISMSE*, **2003**, ESA SP-540, 161-167
16. Heltzel, S. and Semprimoschnig, C. O. A., *Proc. of the 9th ISMSE*, **2003**, ESA SP-540, 179-185